Statistica Neerlandica, MS #2006-44-R1

Statistics for Image Sharpening

Carlo Grillenzoni
University IUAV of Venice
30135 Venezia, Italy
(carlog@iuav.it)

Abstract. Sharpening filters increase the depth of digital images by adding a fraction of their gradient. This portion is tuned by a coefficient which is usually selected according to rules of thumb or subjective evaluation. This paper proposes statistical measures for designing such parameter in a nearly automatic way, avoiding subjective evaluations. The proposed measures are based on the distance between sharpened and equalized images, which serve as an early reference, and test statistics of uniformity of the luminance histogram. More complex measures, based on the trade-off between skewness and kurtosis, and variance and autocovariance of the sharpened image, are also studied. Numerical applications to various kinds of digital images show that the proposed measures provide similar and acceptable solutions.

Key Words. Edge Detection, Equalized Image, Kolmogorov-Smirnov, Image Quality, Pearson-Fisher, Spatial Autoregression, Unsharp Masking.

1. Introduction

Sharpening techniques improve the clearness of digital images by enhancing the marks of the objects which are present in the scene. This improves their borders and their details, giving to the images greater neatness and depth. In general, the strategy of sharpening is to add to the original array a portion of its gradient (e.g. Gonzales and Woods, 2002). This fraction is usually tuned by a coefficient α, which must be properly designed. If the coefficient is not selected adequately, then grain effect and noise are produced also in flat regions, where edges are absent.

Enhancing of images is also pursued by *equalization* and *denosing* methods. Image equalization increases the contrast by flattening the histogram of the pixel luminance, so that all grey levels are represented. There has been recent developments for color images based on curvelet and retinex techniques, e.g. Starck *et al.* (2003) and Funt *et al.* (2004). Image denosing increases the uniformity of flat areas by smoothing on neighboring pixels. Nonparametric statistics has provided effective solutions to the problem of edge-preserving smoothers, e.g. Davies and Kovac (2001), Rue *et al.* (2002), Polzehl *et al.* (2003) and Hillebrand and Müller (2006). However, sharpening differs from these methods because enhances the contrast in the same way as the optical focusing, i.e. by increasing the image depth.

In general, the coefficient α is selected according to rules of thumb or subjective evaluation of the grain side-effect. However, sharpening needs rigorous measures of image quality, as those developed by Avcibas *et al.* (2002) and Bovik *et al.* (2002, 2005). These measures are mostly employed in image compression and restoration to evaluate the goodness of a transformation with respect to the original image. They are also used for comparing denosing methods by blurring the original picture with artificial noises, and then applying the candidate smoothers. A similar approach was also followed by Allebach *et al.* (2005), to design sharpening filters for scanned images, but the reference (ideal) arrays were high-resolution digital photographs. In any event, there is the need for standalone solutions for α, which work fast on the original array and without blurring it artificially. In this context, quality measures can be applied only once a suitable reference image is defined.

In this paper we develop a data-based method to tune the coefficient α without subjective evaluation. The basic strategy consists of using the equalized image as an early reference for the sharpening. This is sensible because equalization increases the contrast without changing the structure of the array, namely the spatial relationships between the pixels. Classical measures of mean absolute and squared distances between sharpened and equalized images can be minimized with respect to α. Moreover, also test statistics based on the histograms, such as Kolmogorov-Smirnov and Pearson-Fisher, can be used. All of these measures are equivalent from a theoretical standpoint, and their empirical results agree.

The main advantage of the proposed solution is the possibility to sharpen images in a fast and automatic way. This can particularly be useful in processing image sequences, as in video recording and transmission. To simplify and robustize the method, the various measures for selecting α can be reduced to the same scale and summarized into a single objective function. Finally, the resulting sharpened images can be further improved through equalization, demonstrating that the two enhancing methods can be fully integrated.

Another important determinant of sharpening is the quality of the gradient image to be added. Classical edge detectors, as those discussed in Bovik *et al.* (1986) and Lim *et al.* (2002), are unsuitable because they only consider positive and significant components of the gradient. Instead, sharpening also needs negative and low signal-to-noise ratio edges. Such components can be obtained even as residuals of spatial auto-regressive (SAR) models (see Tjøstheim, 1983), and in Grillenzoni (2004) adaptive estimators for their parameters are developed.

The quality of sharpening can be significantly improved by adapting the edges to local conditions of contrast. Existing works tend to classify the pixels and to establish specific rules for reducing sharpening in flat areas and only enhancing the others, e.g. Polesel *et al.* (2000), Russo (2005) and Kotera *et al.* (2005). In the final part of this paper, adaptive weights are automatically computed on measures of local relative contrast. Finally, quantitative comparisons of the various solutions are carried out through the ratios of variances of sub-images.

2. Parameter Tuning

2.1 Image Transformations

A digital image consists of a matrix of pixels $\boldsymbol{X} = \{X_{ij}\}$ of size $n_i \times n_j$; in the black and white case, the pixel luminance X is single valued and is usually coded in the set of integers $[0, 255]$. Typical operations of image processing can be viewed as matrix transformations $\boldsymbol{Y} = g(\boldsymbol{X})$. In particular, image compression, denoising and restoration aim to represent the original image in a parsimonious way and to improve its quality. Avcibas *et al.* (2002) and Bovik *et al.* (2002, 2005) have defined several measures for evaluating the quality of a transformation. The most general one combines means $\bar{X}$, $\bar{Y}$, variances σ_X^2, σ_Y^2 and the covariance σ_{XY} as

$$\begin{aligned} Q_{XY} &= \frac{(4\,\sigma_{XY}\,\bar{X}\,\bar{Y})}{(\sigma_X^2 + \sigma_Y^2)\,(\bar{X}^2 + \bar{Y}^2)} \;\in\; (-1, +1) \\ D_{XY}^c &= \frac{1}{n_i\,n_j} \sum_{i=1}^{n_i} \sum_{j=1}^{n_j} \left| X_{ij} - Y_{ij} \right|^c, \quad c = 1, 2 \end{aligned} \tag{1}$$

the quality of $\boldsymbol{Y}$ is good if Q is near 1, and/or the mean distance D is near 0.

These measures also enable to compare the performance of competitive transformations; for example, in the denoising context one has Campbell *et al.* (1990), Davies and Kovac (2001) and Hillebrand *et al.* (2006). In this case, comparisons can be obtained by blurring the original image with an artificial noise $(X_{ij} + v_{ij})$, next computing the denoised image Y_{ij} and then evaluating the indexes (1). The best method is the one which maximizes Q_{XY} or minimizes D_{XY}. Simpler operations, such as optical focusing in digital cameras, only need univariate measures of the recorded image $\boldsymbol{X}$, such as the variance or fourth order moments (e.g. Zhang *et al.*, 1999). The best focal regulation ℓ is that which maximizes the contrast $\sigma_X^2(\ell)$.

Image sharpening consists of adding to the original image a portion of its *edge* $\boldsymbol{E} = \{E_{ij}\}$. It can be represented as the set of linear transformations

$$\begin{aligned} Y_{ij} &= X_{ij} + \alpha\,E_{ij} \\ E_{ij} &= (X_{ij} - M_{ij}) \end{aligned} \tag{2}$$

where M_{ij} is the smoothed image and $\alpha > 0$ is a tuning constant. Typically, $\boldsymbol{M}$ is computed with local means; using a 3×3 window, the equation (2) becomes

$$Y_{ij} = (1+\alpha)\, X_{ij} - \frac{\alpha}{9} \sum_{h=-1}^{1} \sum_{k=-1}^{1} X_{i-h,j-k} \tag{3}$$

If the mean avoids the 4 corner terms $X_{i\pm1,j\pm1}$, and only considers the more adjacent pixels, then the edge coincides with the Laplacian gradient; namely, in the continuous space $E(i,j) = \partial^2 X(i,j)/\partial i\, \partial j$.

To develop the discussion in an effective way, we begin a running example on the testing image "Lena". It is a GIF of size $n_i = n_j = 512$ and range 0-255. Figure 1(a-c) displays sharpened versions obtained with $\alpha = 0, 3, 6$ and a 3×3 averaging window. Apart from the choice of the smoother, the quality of the transformation crucially depends on α. If its value is too high, then "grain effect" is introduced even in flat regions where the gradient is negligible. In general, rules of thumb and subjective evaluation are used for selecting α.

Figure 1. Sharpening of Lena obtained with a 3×3 window and $\alpha = 0, 3, 6$.

2.2 Some Problems

The attempt to select α by means of the strategies commonly used in image processing does not work. As discussed above, best transformations should optimize the quality measures in (1). However, letting $\boldsymbol{Y}(\alpha)$ the sharpened image, one has that $Q_{XY}(\alpha)$ is monotonically decreasing in α and $D^c_{XY}(\alpha)$ are monotonically increasing; see Figure 2(a). Monotonicity is also present in the variance $\sigma^2_Y(\alpha)$ which is used as objective function in auto-focusing. Following the evaluation approach of image denoising, one could replace the original image with the blurred ones

$$X^*_{ij} = \begin{cases} X_{ij} + v_{ij}\,, & v_{ij} \sim \text{Gauss, Uniform, Salt Pepper} \\ \bar{X}_{ij} = (X_{ij} + X_{i-1j} + X_{i+1j} + X_{ij-1} + X_{ij+1})/5 \end{cases}$$

(obtained by adding white noises or smoothing it by local means), and then computing the sharpened image $\boldsymbol{Y}^*(\alpha)$. Unfortunately, also in this case the distances $D^c_{XY^*}(\alpha)$ are monotonically increasing as in Figure 2(a).

To find a measure which is strictly convex or concave in α, one must consider *local* variances of X_{ij}. Thus, let $\boldsymbol{X}^{(1)}$, $\boldsymbol{X}^{(2)}$ be sub-images corresponding to high and low contrast regions. The aim of the sharpening is to increase the variability in the first sub-image *with respect to* the other. It follows that the ratio

$$R_{12}(\alpha) = \text{var}\Big[Y^{(1)}_{ij}(\alpha)\Big]/\text{var}\Big[Y^{(2)}_{hk}(\alpha)\Big] \tag{4}$$

should have a well definite maximum with respect to α. The performance of this measure crucially depends on the choice of the sub-images, which is not an easy task a-priori. Usually, $\boldsymbol{X}^{(1)}$ is placed at the center of the scene, whereas the second one is at the borders; however, in aerial and satellite images the identification of low and high contrast regions may not be possible.

Figure 2 exhibits the path of the statistics (1) and (4) computed on the sharpened version of the Lena image. The sole statistics which has not a monotonic path is (4); it was computed on non-overlapping sub-images of size $n = 100$ placed at the center and at the upper left corner of Figure 1(a). However, the "optimal" value of the parameter is $\alpha = 8$, which is clearly overestimated and unuseful.

Figure 2. Path of statistics (1) and (4) for sharpened versions of the Lena image. (a) Q_{XY}(solid), D_2(dashed); (b) R_{12}(solid), σ^2_Y(dashed); $\alpha = 1, 2 \ldots 20$.

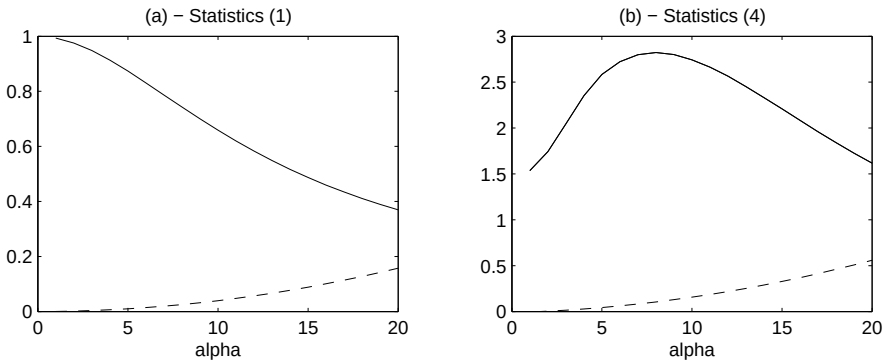

2.3 Some Solutions

In order to define a measure which is strictly convex on the whole image, one must relate $\boldsymbol{Y}(\alpha)$ to an *ideal* array which is different from the original one. The *equalized* image $\boldsymbol{Z}_X = \{Z_{ij}\}$ is the natural candidate because its target is similar to sharpening, but increase the contrast of $\boldsymbol{X}$ by enhancing each grey levels by the same amount. In practice, the probability distribution $f(Z)$ must be Uniform, and this is obtained by standard probability transformations as

$$Z_{ij} = \Big\lfloor F_X(X_{ij})\, 255 \Big\rfloor ; \qquad F_X(k) = \sum_{h=1}^{k} \frac{N_h}{n_i\, n_j}\,, \quad k = 1, 2 \ldots 256$$

where N_k is the frequency of the k-th grey level of the original image, and $F_X(\cdot)$ is the cumulated empirical distribution (see Appendix).

Figure 3 shows the equalized version of the Lena image and its histogram. Figure 3(c) provides the plot of the kernel densities of the sharpened images with increasing values of α

$$f_Y(y_k|\alpha) = \frac{1}{n_i\, n_j\, \kappa} \sum_{i=1}^{n_i} \sum_{j=1}^{n_j} K\left(\frac{Y_{ij}(\alpha) - y_k}{\kappa} \right), \qquad y_k = 0, 1, \ldots 255$$

The above is a sort of smoothed histogram, where $K(\cdot)$ is a density function and $\kappa > 0$ is a smoothing parameter. Under mild conditions, its value can heuristically be designed as $\kappa = \sigma_Y/(n_i\, n_j)^{1/5}$ (see Härdle, 1991).

Figure 3. Comparison of equalization and sharpening: (a) Equalized image $\boldsymbol{Z}$; (b) Its frequency histogram; (c) Kernel densities $f_Y(y_k)$ of sharpened images with α = 0 (bold dot), 3 (solid), 6 (dashed), 9 (dot dashed).

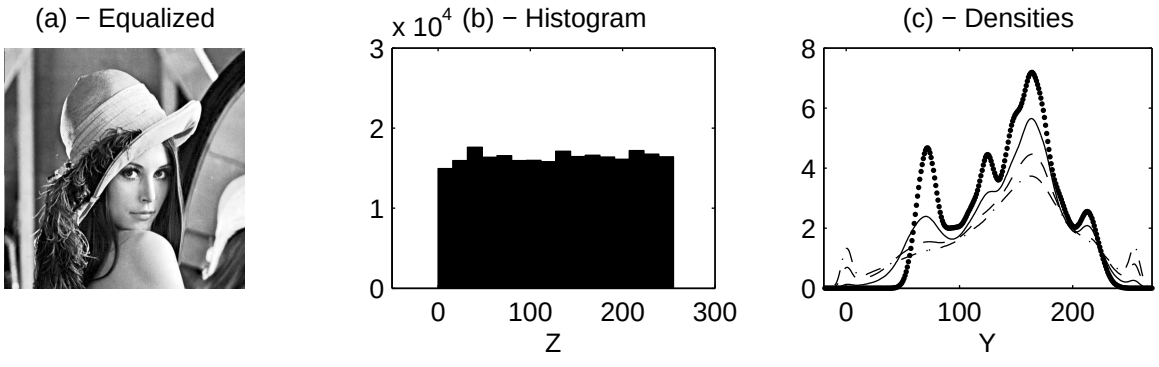

Because equalization and sharpening have a similar target, but pursue it in independent ways, the distance measure $D^c_{ZY}(\alpha)$ should have a well definite minimum in α. Therefore, a reasonable selection strategy becomes:

$$\alpha_{\text{opt}} = \arg\min_{\alpha} \; D_c\Big(\boldsymbol{Z}_X, \boldsymbol{Y}(\alpha)\Big), \quad c = 1, 2 \tag{5}$$

Analogously, one can minimize test statistics which directly compare the distribution function of $Y_{ij}(\alpha)$ with the Uniform one, such as those of Kolmogorov-Smirnov (KS) and Pearson-Fisher (PF) (e.g. see Dudewicz and Mishra, 1988)

$$\begin{aligned} S_1(\alpha) &= \sqrt{n_i\, n_j}\, \sup_k \Big| F_{Y(\alpha)}(k) - k/256 \Big| \\ S_2(\alpha) &= \sum_{k=1}^{256} \left(\frac{N_k(\alpha)}{n_i\, n_j} - \frac{1}{256} \right)^2 256 \end{aligned} \tag{6}$$

where $N_k(\alpha)$ is the absolute frequency of the k-th grey level of the sharpened image. The second statistics (PF) is more robust and convex with respect to the KS one because it uses the sum operator and the squared value.

Another measure which has a convex pattern with respect to α is the skewness-kurtosis (SK) statistic defined by Bera and Jarque (1982) for testing Gaussianity in time series. Adapting it to spatial series, it becomes

$$S_3(\alpha) = \frac{n_i\, n_j}{6} \left[\left(\frac{\mu_3(\alpha)}{\sigma_Y^3} \right)^2 + \frac{1}{4} \left(\frac{\mu_4(\alpha)}{\sigma_Y^4} - 3 \right)^2 \right] \tag{7}$$

where $\mu_c(\alpha) = \mathrm{E}\Big[\, Y_{ij}(\alpha) - \mu_Y \Big]^c$ are central moments of order $c > 0$. To understand the meaning of such statistic, consider Figure 3(c): it shows that as α increases, symmetry and unimodality of the probability density improve, but its flatness and dispersion worsen. This means that the indexes of skewness (μ_3/σ^3) and kurtosis (μ_4/σ^4) have an opposite behavior with respect to α. The statistic (7) then realizes a compromise between the two opposite tendencies and, therefore, can have a well definite minimum.

Notice that in data analysis, the above statistics are used for testing hypotheses of Uniform and Normal densities. Under these assumptions and the independence condition, it can be shown that their distribution is of χ^2 type. However, in our context they mostly serve as objective functions for selecting α.

Figure 4. Path of statistics (5)-(7) for sharpened versions of the Lena image: (a) D_2(solid), D_1(dashed); (b) S_3(solid), S_1(dashed); where $\alpha = 0, 0.5, 1 \ldots 5$.

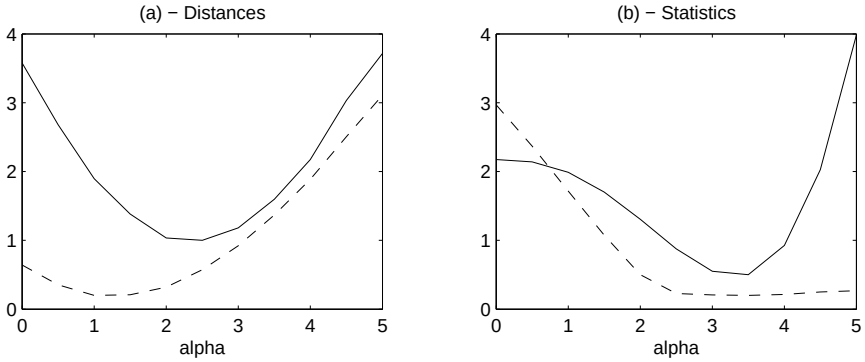

Figure 4 provides the path of the statistics (5)-(7) applied to sharpened version of the Lena image. Their values was rescaled for the sake of representation. Panel (a) provides the mean distances D^c_{ZY} and the panel (b) exhibits the KS and SK measures. Unlike the Kolmogorov-Smirnov statistic, there are well definite convex paths, and the optimal value of α is placed in the set (2.5, 3.5). The important feature is that this interval is narrow and constituted by mild and acceptable values. Further, it is stable on resizing, rescaling and partitioning the original image, such as working on the central part of it, as $\boldsymbol{X}^{(1)}$.

2.4 Strong Evidence

In this sub-section we massively test the previous solutions for α, by sharpening digital images of various nature, such as satellite, aerial, microscope, X-rays, magnetic resonance, etc.. Many of the images were downloaded from the Internet site of the book by Gonzales and Woods (2002). Low resolution images and numerical values of the rescaled statistics are displayed in Figure 5.

In general, the displayed measures have a convex pattern, although they are not alway smooth (i.e. differentiable); moreover, they provide values in the narrow interval (1,3). To obtain a single value, one can consider the *global* objective function given by the sum of the standardized statistics: $J_m(\alpha) = \sum_{k=1}^{m} \Big(S_k(\alpha) - \hat{\mu}_k \Big) / \hat{\sigma}_k$, where means and variances are computed over the values of $S(\alpha_h)$.

Figure 5. Path of the statistics (5)-(7) for sharpened versions of various images. (a) Aerial of WTC-911; (b) City from LandSat; (c) Hurricane from NOAA; (d) Finger print; (e) Hant head; (f) Electronic microscope; (g) Virus cells; (h) Radiography; (i) Magnetic resonance (MRI); (j) Peppers; (k) Mandrill; (l) Barbara. Statistics in the headings are listed in the following order: Solid, Dashed, Dash-Dot.

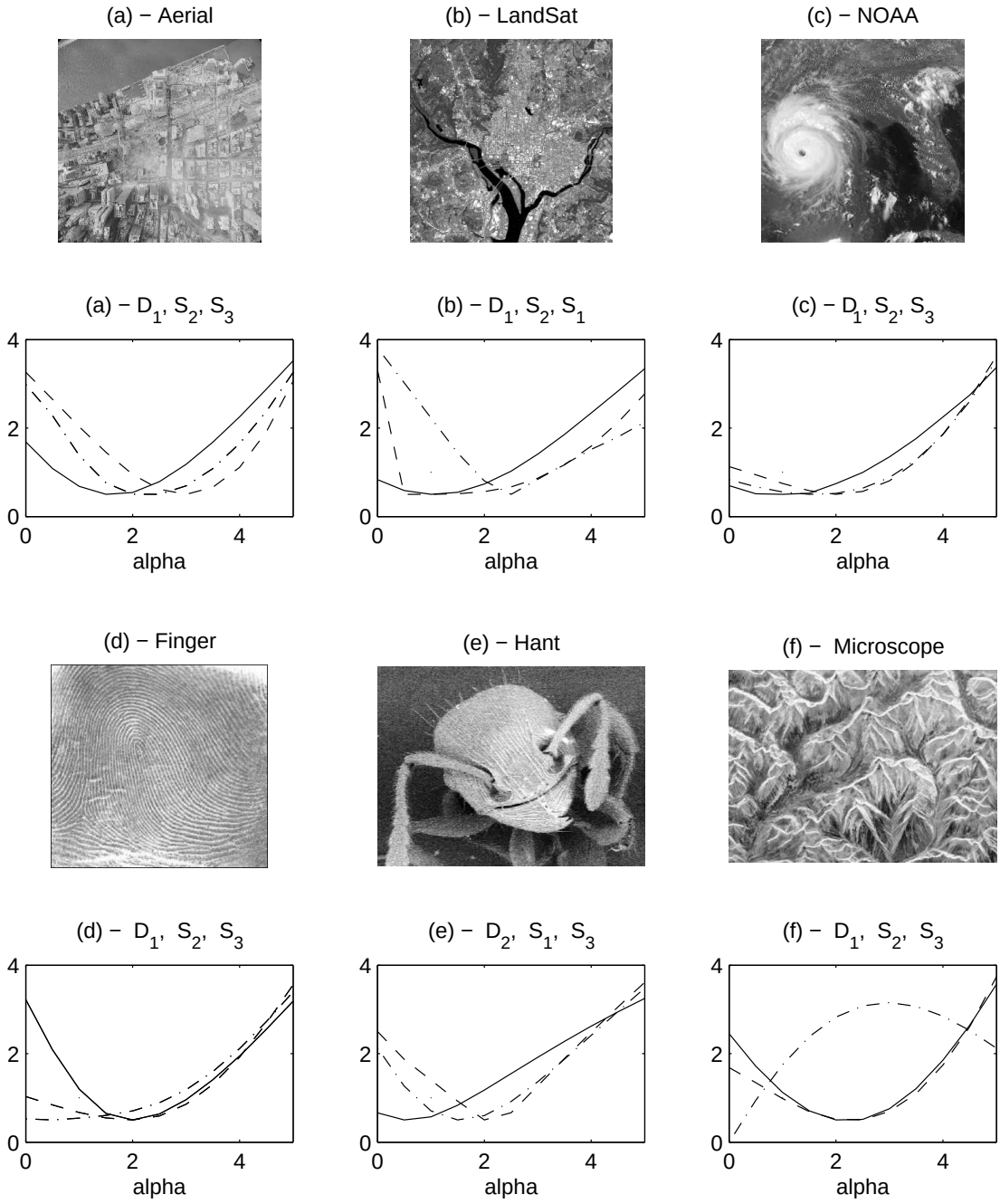

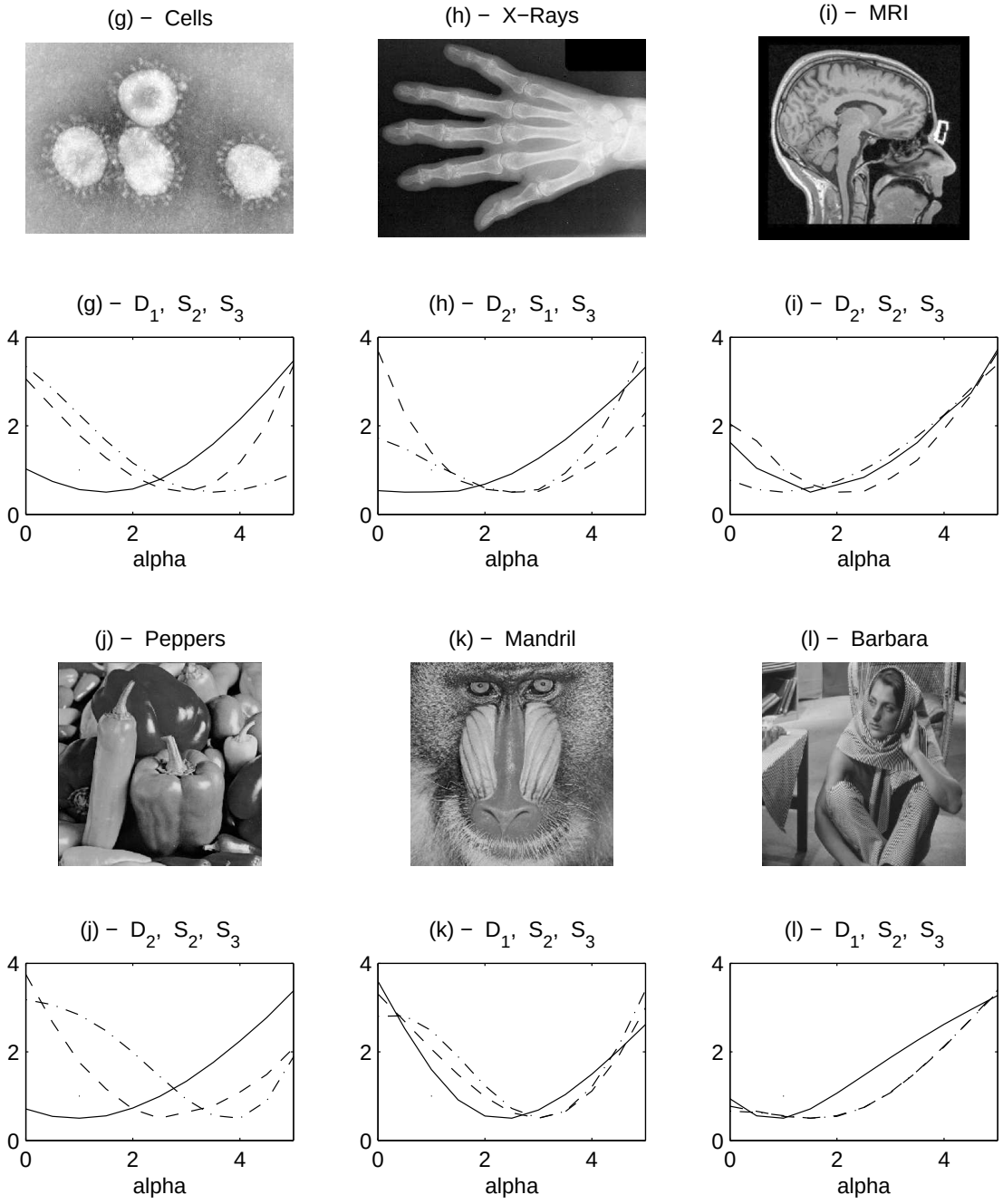

By definition, the proposed method works well on images which have a rich texture (i.e. a high variability). In the presence of extended flat regions (such as in X-ray, MRI and Microscope images), the statistics must be computed on suitable areas. By default, one can choose the central part of the image having a size at least 1/3 of the original array. The most stable and convex measures are D_1 (the mean absolute distance) and S_2 (the Pearson-Fisher statistic); they must be preferred in

real-life applications. The basic philosophy of the outlined strategy is to consider equalization as an early reference for sharpening. However, one can also integrate the two techniques by equalizing the final sharpened image.

2.4 A Special Solution

Previous statistics work well, but do not consider the spatial dependence between pixels. Indicators of dependence are given by the spatial auto-covariances (ACV): $\gamma_X(h,k) = \mathrm{E}(X_{ij}X_{i-h,j-k}) - \mu_X^2$, which measure the relationship of cells which are separated by h-rows and k-columns. Now, because the sharpening reduces smoothness, it also reduces the auto-correlation (ACR): $\rho_Y(h,k) = \gamma_Y(h,k)/\sigma_Y^2$. This is shown in Figure 6(b), as regards the Lena image and the lags $k = h$; indeed, as α increases, $\rho_Y(k = h)$ decreases for all k.

On the other hand, it is known that sharpening increase the variance $\sigma_Y^2 = \gamma_Y(0,0)$; therefore, a statistic which sums Var and ACV should have a maximum point in α. Using unbiased estimates and a common lag $h = k$, one can define

$$S_4(\alpha|m) = \sum_{k=(0,1)}^{m} \left[\hat{\gamma}_Y(k) = \frac{1}{(n_i - k)(n_j - k)} \sum_{i=k+1}^{n_i} \sum_{j=k+1}^{n_j} (Y_{ij} - \bar{Y})(Y_{i-k,j-k} - \bar{Y}_{-k}) \right] \tag{8}$$

where m is the maximum lag, and $\bar{Y}_{-k}$ is computed on $i, j = (k+1) \ldots n_i,\, n_j$.

Figure 6. Spatial dependence of Y_{ij}, $Y_{i-k,j-k}$ in sharpened versions of the Lena images with $0.05 \leq \alpha \leq 7.5$: (a) Autocovariances $\hat{\gamma}_Y(k,k)$; (b) Autocorrelations $\hat{\rho}_Y(k,k)$; with $k = 0, 1, 2, 4, 6 \ldots 40$ (even for $k > 1$).

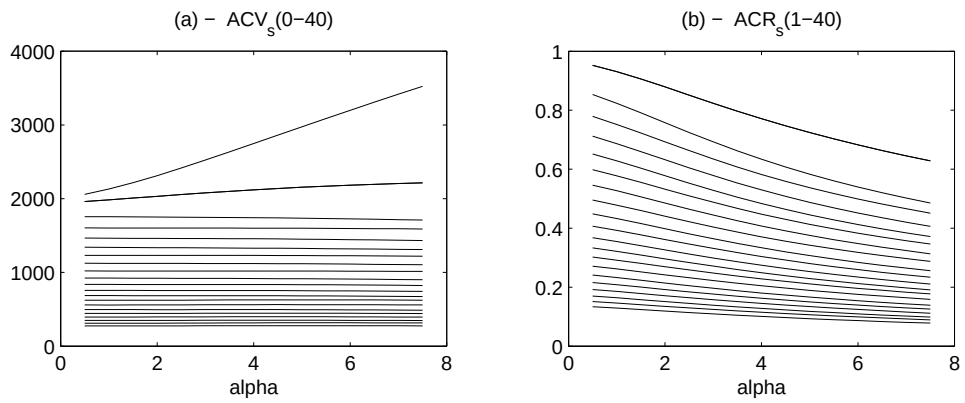

In order to render strictly concave the statistic S_4, it may be necessary to start the first sum in (8) with $k=1$ because the filter (3) includes the term $X_{i-1,j-1}$. In fact, this inclusion renders the first autocovariance $\gamma_Y(1)$ increasing in α, that is a substitute for the variance $\gamma_Y(0)$, see Figure 6(a). Moreover, because the autocovariance values depend on the texture of the image, the lag k could be defined only by row (with $Y_{i-k,j}$) or by column (with $Y_{i,j-k}$). Figures 7(a,b) show the behavior of the statistic (8) with these specifications. They provides indications which are consistent with the previous measures in Figure 4; moreover, they have the advantage of taking into account the stochastic dependence between pixels.

Figure 7. Pattern of the statistic (8) with $m = 20$ in sharpened versions of Lena image: (a) S_4 as a function of $\hat{\gamma}_Y(0,k)$; (a) S_4 as a function of $\hat{\gamma}_Y(h,0)$.

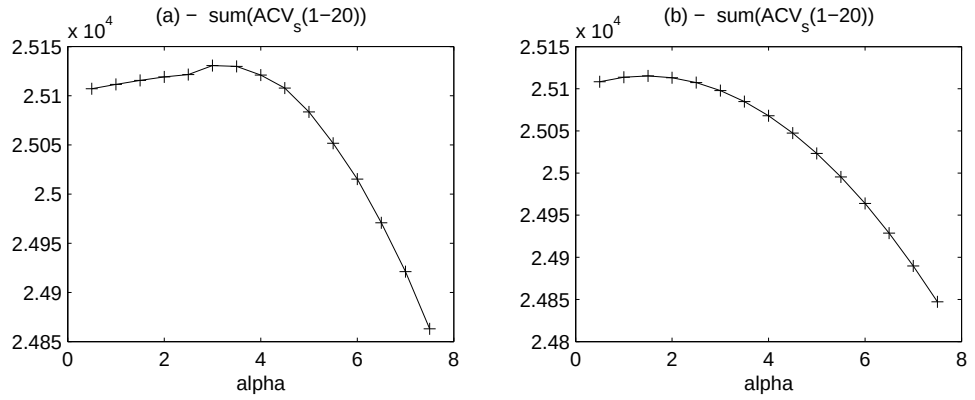

The general feature of the statistics S_3-(7) and S_4-(8) is to establish a trade-off between two *incompatible* cost (gain) function, so that the resulting objective function should have a well definite minimum (maximum) point. Although the nature of these solutions is heuristic, the remarkable fact is that they indicate values for α which are close to those of the measures based on the equalized image. The main weakness of S_3 is the possible lack of convexity (see Figure 5(f)), and the problems of S_4 are the computational complexity and non-automaticity.

3. Adaptive Sharpening

3.1 Edge Estimation

The quality of the sharpening also depends on the estimation of the edge E_{ij}. This issue must not be confused with the problem of *edge detection*, which concerns with positive and significant components. The array $\boldsymbol{E}$ in (2) is more complex, and also includes elements with negative sign or with low signal-to-noise ratio. To be specific, consider the detector discussed in Bovik *et al.* (1986) and Lim *et al.* (2002); it is based on the mean difference of symmetric partitions of regular windows, as

$$\begin{pmatrix} X^L_{11} & X^L_{12} & X^R_{13} \\ X^L_{21} & \cdot & X^R_{23} \\ X^L_{31} & X^R_{32} & X^R_{33} \end{pmatrix}, \quad \begin{pmatrix} X^A_{11} & X^A_{12} & X^A_{13} \\ X^B_{21} & \cdot & X^A_{23} \\ X^B_{31} & X^B_{32} & X^B_{33} \end{pmatrix}$$

$$U_{ij} = \max\left(\left| \bar{X}^L_{ij} - \bar{X}^R_{ij} \right|, \left| \bar{X}^A_{ij} - \bar{X}^B_{ij} \right| \right) \tag{9}$$

where $\bar{X}^L_{ij} = (X_{i-1j-1} + X_{i-1j} + X_{ij-1}X_{i+1j-1})/4$ and so on. The estimator (9) becomes an edge detector by testing the significance of each U_{ij} with classical T-statistics (e.g. Dudewicz and Mishra, 1988).

On the basis of (9), it follows that a simpler detector can just be obtained by subtracting to each pixel the *smallest* one of its neighboring values. More generally, one can define positive and negative edges as follows

$$\begin{aligned} E^+_{ij} &= X_{ij} - \min(X_{i\pm1,j\pm1}) \\ E^-_{ij} &= X_{ij} - \max(X_{i\pm1,j\pm1}) \\ E^*_{ij} &= E^+_{ij} + E^-_{ij} \end{aligned} \tag{10}$$

the latter defines an edge estimator which is suitable for sharpening. In particular, it is more sensitive than that used in the previous section because, on the Lena image, it has a variance σ^2_E which is 10 times greater than that in (3).

Figure 8 compares the estimators (9)-(10) on the Lena image, and evaluates their effect on the sharpening with $\alpha = 2$. It confirms that edge detection and edge estimation for sharpening are different issues; in particular, the first only concerns with positive components and selects the most significant ones.

Figure 8. Edge estimation and sharpening: (a,b) Solution (9); (c,d) Solution (10).

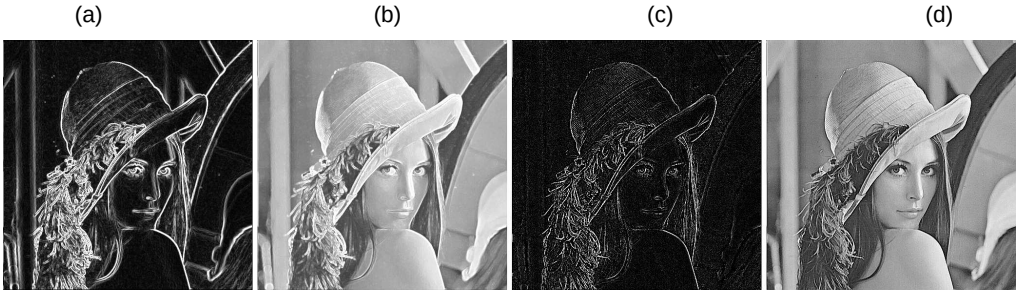

3.2 Spatial regression

A full statistical approach to edge estimation is based on spatial auto-regressive (SAR) models. These schemes exploit the dependence between pixels and estimate the edges in terms of *residuals* of regression. The first-order model is given by

$$X_{ij} = \phi_1 X_{i,j-1} + \phi_2 X_{i-1,j} + \phi_3 X_{i-1,j-1} + \ldots + \phi_8 X_{i+1j+1} + E_{ij} \qquad (11)$$

where $\{\phi_l\}_1^8$ are coefficients to be estimated. With respect to the filter (3), where ϕ_l=1/9 for all l, the adaptivity of the system (11) is apparent.

Under conditions of stationarity one has $\gamma(h,k) = \gamma(-h,-k)$, and the right hand side of (11) can be reduced to the first 3 terms only. This constraint is named *causal* and enables the *parametric identifiability* of the model (11) (see Tjøsteim, 1983); in practice, it allows the parameter estimates to be consistent. Thus, letting $\boldsymbol{\phi} = [\,\phi_1,\, \phi_2,\, \phi_3\,]'$ and $\boldsymbol{x}_{ij} = [\,X_{i,j-1},\, X_{i-1,j},\, X_{i-1,j-1}\,]'$, the causal model can be written as $X_{ij} = \boldsymbol{\phi}'\,\boldsymbol{x}_{ij} + E_{ij}$, and the least-squares (LS) estimator becomes

$$\hat{\boldsymbol{\phi}}_{\mathrm{LS}} = \arg\min_{\phi} \sum_{i=2}^{n_i}\sum_{j=2}^{n_j} E_{ij}^2(\boldsymbol{\phi}) = \left(\sum_{i=2}^{n_i}\sum_{j=2}^{n_j} \boldsymbol{x}_{ij}\boldsymbol{x}_{ij}'\right)^{-1} \sum_{i=2}^{n_i}\sum_{j=2}^{n_j} \boldsymbol{x}_{ij} X_{ij} \qquad (12)$$

Application of (12) to the Lena image provided $\hat{\boldsymbol{\phi}}_{\mathrm{LS}} = [\,.57,\, .84,\, -.42\,]'$; with this, one can generate the residuals $\hat{E}_{ij} = X_{ij} - \hat{\boldsymbol{\phi}}_{\mathrm{LS}}'\,\boldsymbol{x}_{ij}$, which provide the edges for the sharpening. The coefficient α can be designed with the same strategies as Section 2, namely with the statistics (5)-(8). Numerical results are similar to those in Figure 4 and 7, and indicate α=3. The resulting sharpened image is similar to Figure 8(d), and improves that of the filter (3).

The adaptive capabilities of SAR models can be improved by applying *local* estimation techniques. These methods enable to obtain parameter estimates $\hat{\boldsymbol{\phi}}_{ij}$ which adapt to local conditions of contrast and texture of the image. Following Grillenzoni (2004), a simple algorithm can be obtained from (12) by weighting the regressors with exponentially decaying weights

$$\hat{\boldsymbol{\phi}}_{ij} = \left(\sum_{h=2}^{n_j} \sum_{k=2}^{n_j} \lambda_1^{|i-h|} \lambda_2^{|j-k|} \, \boldsymbol{x}_{hk} \, \boldsymbol{x}'_{hk} \right)^{-1} \sum_{h=2}^{n_i} \sum_{k=2}^{n_i} \lambda_1^{|i-h|} \lambda_2^{|j-k|} \, \boldsymbol{x}_{hk} \, X_{hk} \qquad (13)$$

where $0 < \lambda_1, \lambda_2 \leq 1$ are coefficients of spatial adaptivity.

Constraining $\lambda_1 = \lambda_2$, the resulting coefficient can be designed with bivariate forms of the statistics (5)-(8). With respect to the Lena image, $S_2(\alpha, \lambda)$ attains a minimum at the point (3,.7). Anyway, given α, the quality of sharpened images is relatively insensitive to the choice of λ, and seems worst than that in Figure 8(d). Figure 9 displays the estimates $\hat{\boldsymbol{\phi}}_{ij}(\lambda)$ obtained with a mild value of λ.

Figure 9. Local estimates (13) of SAR parameters obtained with $\lambda_{1,2} = 0.9$.

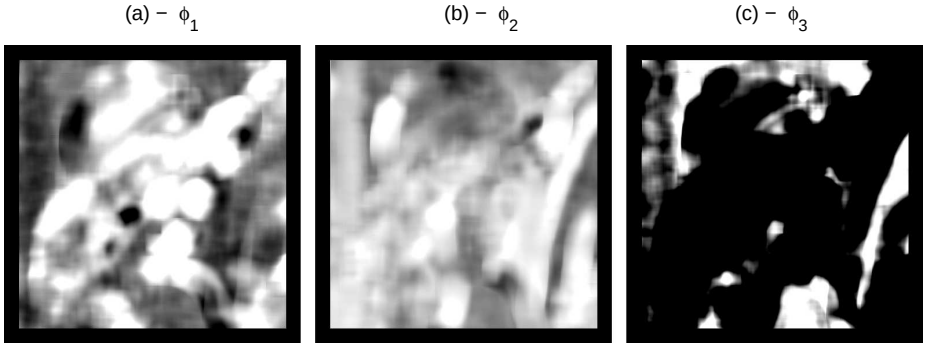

3.3 Adaptive edges

The filters we have discussed so far: (2), (10), (13) have the undesirable side-effect of enhancing all noise components, also in flat regions where the gradient is negligible. To improve the image significantly, it is necessary to intervene on the mechanism of sharpening itself, by selecting the edges (residuals) to be added. A sensible approach is the opposite one of *robust* statistical methods, and consists of rejecting small residuals and accepting the largest ones. In this way, uniform regions would be preserved from noise and only contrasted regions would be enhanced, see

Polesel *et al.* (2000), Russo (2005) and Kotera *et al.* 2005).

In general, it is also possible to improve the smoothness of flat areas by replacing the original pixels with the smoothed ones $\hat{X}_{ij} = \hat{\boldsymbol{\phi}}'_{\mathrm{LS}} \boldsymbol{x}_{ij}$. Thus, using the indicator function $I(\cdot)$, the *integrated* sharpening-smoothing filter becomes

$$Y_{ij} = X_{ij} + \alpha\, I\Big(|\hat{E}_{ij}| > \delta\, \hat{\sigma}_E\Big)\, \hat{E}_{ij} - I\Big(|\hat{E}_{ij}| \leq \delta\, \hat{\sigma}_E\Big)\, \hat{E}_{ij} \tag{14}$$

which follows by $\hat{E}_{ij} = (X_{ij} - \hat{X}_{ij})$. Under Gaussianity the threshold coefficient should be $\delta = 2, 3$; however, the density of E_{ij} usually has heavy tails and it must be larger. In general, it is difficult to tune δ automatically and the filter (14) tends to smooth low-medium edges and to produce sparse outliers.

To avoid these drawbacks, it is necessary to adapt the edges to the local conditions of relative variability in the original image. An automatic solution, with spatially varying α-weights is given by

$$\begin{aligned} Y^*_{ij} &= X_{ij} + \hat{\alpha}_{ij}\, E_{ij}\,, \quad \hat{\alpha}_{ij} = \alpha \left[\frac{\hat{\sigma}_{ij}}{\max(\hat{\sigma}_{ij})}\right] \\ \hat{\sigma}^2_{ij} &= \frac{1}{(2d+1)^2} \sum_{h=-d}^{d} \sum_{k=-d}^{d} (X_{i-h,j-k} - \bar{X}_{ij})^2 \end{aligned} \tag{15}$$

where $\hat{\sigma}^2_{ij}$ and $\bar{X}_{ij}$ are local estimates obtained with a $(2d{+}1)$ square window, with $d \geq 1$. The rationale of (15) is to tune the edges proportionally to the local contrast; specifically, because $\alpha_{ij} \leq \alpha$, flat regions are preserved from noise and outliers, while contrasted regions have weights near α.

The parameter α of (15) can be selected as in Section 2; however, from a visual standpoint the filter has shown less sensitivity to such coefficient with respect to previous methods. Figure 10(a) plots the weights $\hat{\alpha}_{ij}$ with d=3, placed in increasing order, and Figure 10(b) shows the path of the statistics (5)-(7). To improve the sensitivity of (15) to low-medium contrast, the profile of $\{\alpha_{ij}\}$ can be made less sharp by using α^{γ}_{ij}, $0 < \gamma < 1$. Finally, Figure 10(c) provides the sharpened image obtained with the edge estimator (10) and the coefficients $\alpha = 5$, $\gamma = 0.5$. Without doubts, its quality is significantly better than those in Figures 1(b) and 8(d).

Figure 10. Elements of the filter (15): (a) Weights $\hat{\alpha}_{ij}$ and $\hat{\alpha}_{ij}^{1/2}$ (dashed); (b) Statistics (5)-(7); (c) Sharpened image with edge (10) and $\alpha = 5$.

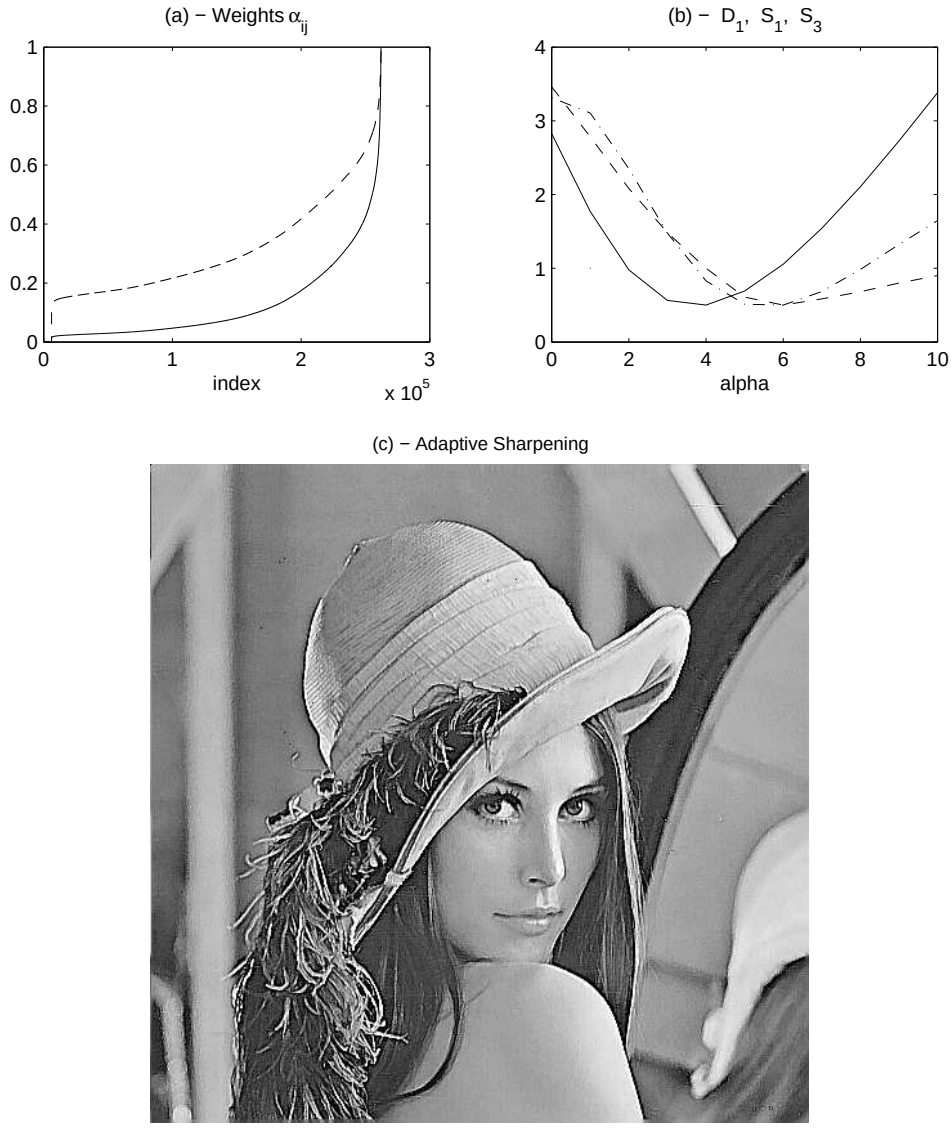

3.4 Comparisons

In the previous sections we have discussed several methods of edge estimation and image sharpening, e.g. (3) is based on mean values, (9) uses a mean-difference edge-detector, (10) sums positive and negative edges, (11) considers residuals of regression, (15) follows an adaptive weights strategy. Apart from subjective preferences, the question is: How to evaluate their performance objectively ?

Un answer comes from the relative variance (4). As we saw, it is unsuitable for

selecting α, but now it can be used to compare alternative methods. Given regions with low and high variability, the best sharpening is the one which maximizes the statistic R_{12}. With respect to the Lena image, we selected 3 disjoint sub-images of size 100×100, placed on the main diagonal, starting from the upper-left corner. These correspond to low, medium and high contrast areas; namely $\boldsymbol{X}^{(3)}$ is nearly flat, $\boldsymbol{X}^{(2)}$ contains the head, $\boldsymbol{X}^{(1)}$ includes the eyes. We made double comparisons: high/medium and medium/low, and results are summarized in Table 1.

Several remarks are in order. First column reports the statistic (4) for the original image; notice that the ratio $R_{23} < 1$, so that it seems that $\boldsymbol{X}^{(2)}$ is less contrasted than $\boldsymbol{X}^{(3)}$. In reality, all of the sharpening methods provide $R_{23} > 1$. The edge-detection method (9) gives the worst result, especially in terms of the global statistic $R_{12} + R_{23}$; this confirms the importance of negative edges. Despite of their computational complexity and elegance, the performance of the spatial regression methods (12)-(13) are similar to the classical ones (2)-(3). The modified method (10)" corresponds to $E_{ij}^{**} = \text{sign}(E_{ij}^{*}) \max(E_{ij}^{+}, -E_{ij}^{-})$, and actually improves (10). The adaptive solutions (15) outperform the others and their global statistic is much greater than that of the original image. Their performance can be further improved with refinement of the adaptive weights and edges.

Table 1. Statistics (4) for various sharpening methods computed on 3 sub-images of Lena (they have size 100×100 and are placed on the main diagonal).

Method	Orig.	(3)	(9)	(10)	(10)"	(12)	(13)	(15)+(3)	(15)+(10)
R_{12}	4.38	3.47	2.47	3.72	3.53	3.54	3.38	3.85	4.37
R_{23}	0.66	1.05	1.10	1.11	1.55	1.21	1.24	1.97	2.53
Sum	5.04	4.53	3.57	4.83	5.08	4.75	4.62	5.82	6.90

We conclude the section by applying the adaptive sharpening (15)+(10) to other testing images taken from Gonzales and Woods (2002). Results are reported in Figure 11, where they are compared with the sharpening function of the MATLAB package. Differences can be appreciated by enlarging the images, which shows the

greater noise of the Matlab solution. Moreover, the mean value of the variance ratio R_{YX} (computed on the five images), is 1.34 for Matlab and 2.13 for the method (15). This means that the adaptive approach achieves a greater signal-to-noise ratio.

Figure 11. Comparison of the sharpening function of Matlab and the adaptive sharpening (15)+(10) for various classes of images; (please zoom on the panels).

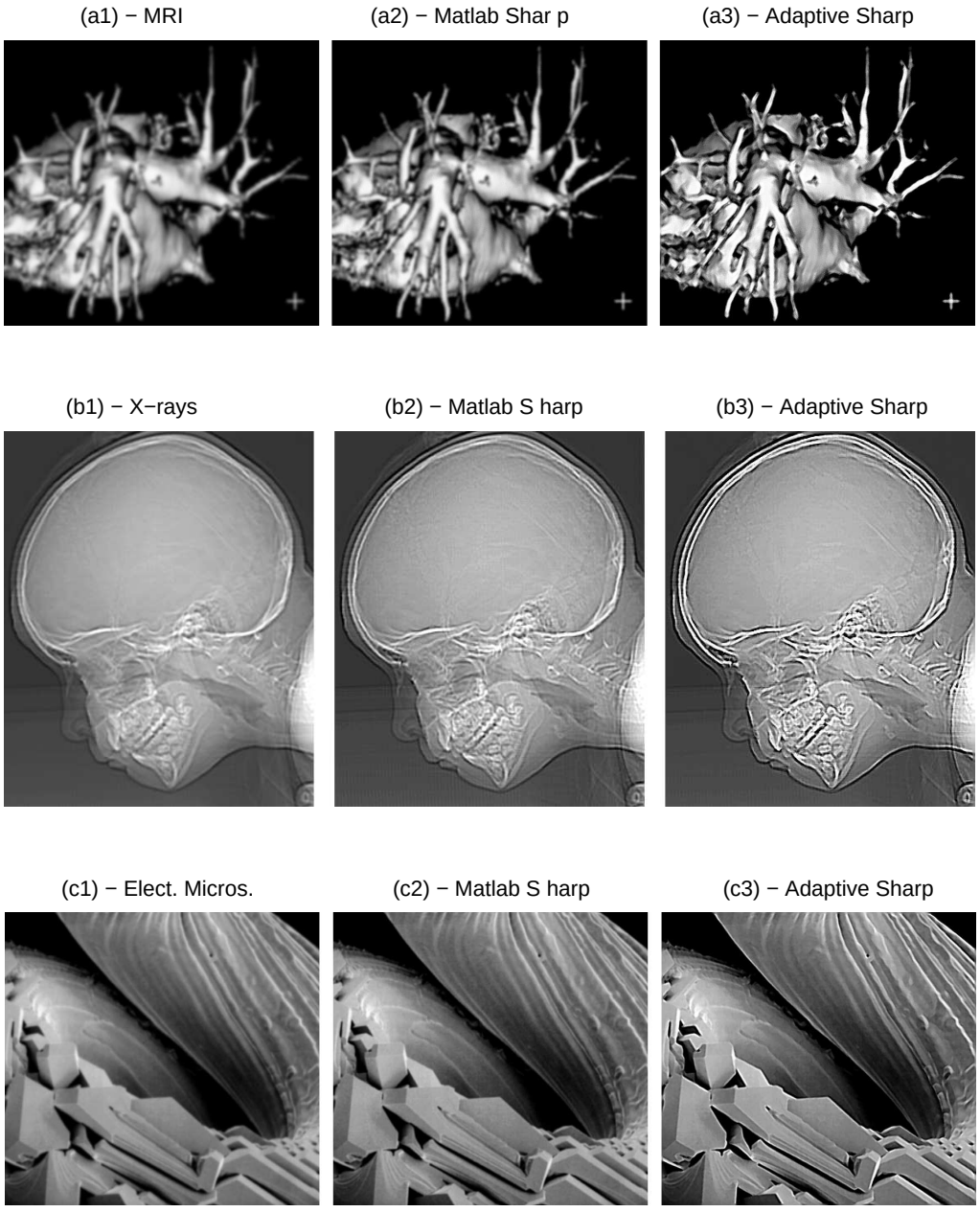

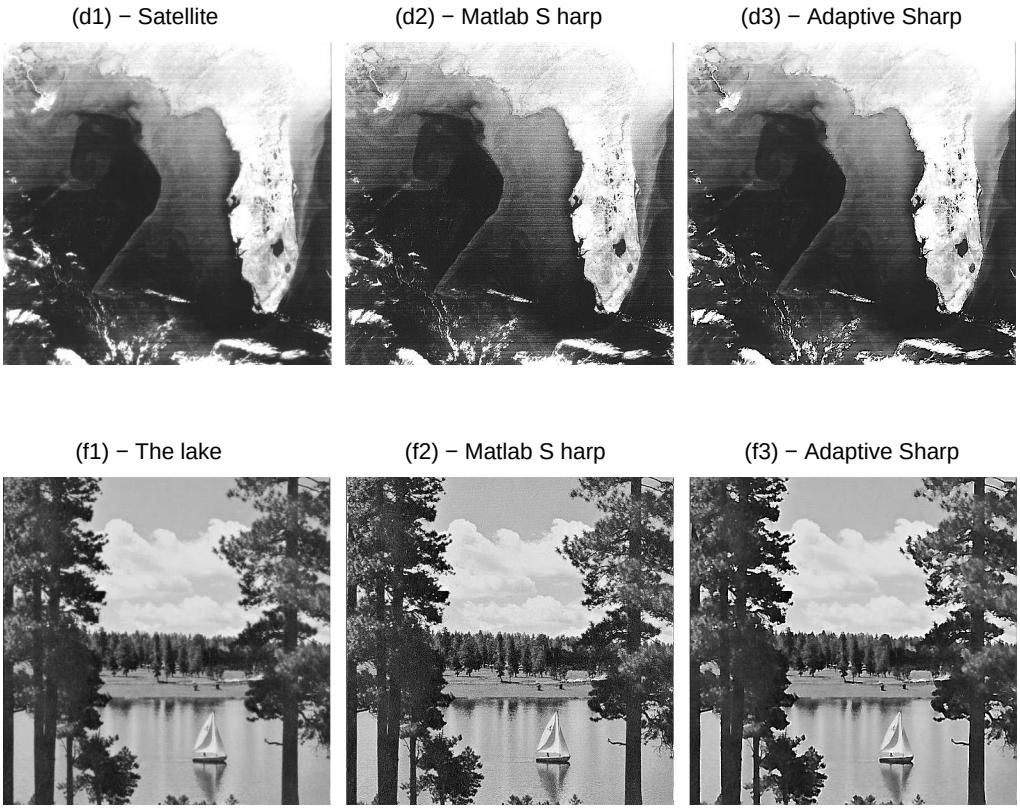

4. Conclusions

In this paper we have discussed statistical methods for digital image enhancement. The two main contributions have been: i) new statistical measures for the design of the sharpening parameter α; and ii) new adaptive techniques for the estimation and the tuning of the edge component $\boldsymbol{E}$.

In the first part, we have considered several statistics which relate the sharpened image to the equalized one, which serves as a benchmark. These measures are direct, as the mean absolute and quadratic distances, or indirect, as the Kolmogorov-Smirnov and Pearson-Fisher statistics for testing the hypotheses of uniform distribution. Furthermore, we also have considered complex measures based on higher order moments (skewness, kurtosis, autocovariance, etc.) that are suitable for analyzing the effects of α. All of these measures tend to behave in a strict convex way with respect to the tuning parameter. By standardization and summation, a global

objective function can be achieved, which can lead to a unique solution. Numerical experiments, carried out on various images, have shown the validity of the approach; in particular, they have provided mild and similar values.

In the second part, we have changed the classical structure of sharpening filters. In particular, the edges based on mean values have been replaced by residuals of auto-regression models and by adaptive sums of positive and negative edges. Local estimators for causal SAR models have been developed and their practical usage is demonstrated. We have also developed an adaptive approach for tuning sharpening weights on the basis of the local relative variability. This concretely solves the problems of grain effect and noise diffusion which are present in classical techniques. Also in this case, numerical applications on known testing images have shown the validity of the proposed solutions.

Appendix

In this Appendix we briefly review the proof of the equalization formula $Z_{ij} = \left\lfloor F_X(X_{ij})\, 255 \right\rfloor$ that was introduced in Section 2.3. For a grey scale defined on the unit interval $x \in (0,1)$, equalization consists of finding a single valued monotonically increasing transformation $z = t(x)$ such that $f_z(z) = 1$ for all $z \in (0,1)$. Using the properties of probability densities, one has $f_z(z) = f_x(x)\mathrm{d}x/\mathrm{d}z$, and substituting $f_z(z) = 1$ and $z = t(x)$, it follows that $\mathrm{d}t(x)/\mathrm{d}x = f_x(x)$. By integration, the required solution becomes $t(x) = \int_0^x f_x(u)\,\mathrm{d}u = F_x(x)$, which is the cumulated probability. Now, returning to a $n_i \times n_j$ real image with discrete grey levels $X_k = 0, 1, 2 \ldots 255$, one has $f_X(X_k) = N_k/(n_i\, n_j)$, where N_k is the absolute frequency of X_k. Hence, using the transformation one has $Z_k = t(X_k) = \sum_{h=1}^{k} N_h/(n_i\, n_j) = F_X(X_k)$. Finally, applying this to any pixel and rescaling and rounding the values, one has the formula stated at the beginning.

References

Allebach J.P. and Kim S.-H. (2005), Optimal unsharp mask for image sharpening and noise removal. *Journal of Electronic Imaging*, **14**, 1-13.

Avcibas I., Sankur B. and Sayood K. (2002), Statistical evaluation of image quality measures. *Journal of Electronic Imaging*, **11**, 206-223.

Bera A.K. and Jarque C.M. (1982), Model specification tests: a simultaneous approach. *Journal of Econometrics*, **20**, 59-82.

Bovik A.C., Huang T.S. and Munson D.C. (1986), Nonparametric tests for edge detection in noise. *Pattern Recognition*, **19**, 209-219.

Bovik A.C. and Wang Z. (2002), A universal image quality index. *IEEE Signal Processing Letters*, **9**, 81-84.

Bovik A.C., Simoncelli A. and Wang Z. (2005), Structural Approaches to Image Quality Assessment; in *Handbook of Image and Video Processing*, A.C. Bovik, Ed.. Academic Press, New York.

Campbell T.G. and Du Buf J.M. (1990), A quantitative comparison of edge preserving smoothing techniques. *Signal Processing*, **21**, 289-301.

Chu C.K., Glad I., Godtliebsen F. and Marron J.S. (1998), Edge-Preserving Smoothers for Image Processing. *Journal of American Statistical Association*, **93**, 526-541.

Davies P.L. and Kovac A. (2001), Local extremes, runs, strings and multiresolution (with discussion). *Annals of Statistics*, **29**, 1-65.

Dudewicz E.J. and Mishra S.N. (1988), *Modern Mathematical Statistics*. J. Wiley, New York.

Funt B., Ciurea F. and McCann J. (2004), Retinex in Matlab. *Journal of Electronic Imaging*, **13**, 48 57.

Gonzalez, R.C. and Woods, R.E. (2002). *Digital Image Processing*, 2nd ed. Prentice Hall, Upper Saddle River (NJ).

Grillenzoni C. (2004), Adaptive spatio temporal models for satellite ecological data. *Journal of Agricultural, Biological and Environmental Statistics*, **9**, 158-180.

Guillon S., Baylou P., Najim M. and Keskes N. (1998), Adaptive nonlinear filters for 2D and 3D image enhancement. *Signal Processing*, **67**, 237-254.

Härdle W. (1991), *Smoothing Techniques: with Implementation in S*. Springer: Berlin.

Hillebrand M. and Müller C. (2006), On consistency of redescending M-kernel smoothers. *Metrika*, **63**, 71-90.

Lim D.H. and Jang S.J. (2002), Comparison of two-sample tests for edge detection in noisy images. *The Statistician*, **51**, 21-30.

Kotera H., and Wang H. (2005), Multi-Scale Image Sharpening Adaptive to Edge Profile. *Journal of Electronic Imaging*, **14**, 1-13.

Polesel A., Ramponi G. and Mathews J. (2000), Image enhancement via adaptive unsharp masking. *IEEE Transactions on Image Processing*, **9**, 505-510.

Polzehl J. and Spokoiny V. (2003), Image Denoising: Pointwise Adaptive Approach. *Annals of Statistic*, **31**, 30-57.

Rue H., Chu C.-K., Godtliebsen F. and Marron J.S. (2002), M-smoother with local linear fit. *Journal of Nonparametric Statistic*, **14**, 155-168.

Russo F. (2005), Automatic enhancement of noisy images using objective evaluation of image quality. *IEEE Trans. on Instrumentation and Measurement*, **54**, 1600-1606.

Starck J.L., Murtagh F., Candes E.J. and Donoho D.L. (2003), Image contrast enhancement by curvelet transform. *IEEE Transactions on Image Processing*, **12**, 706-717.

Tjøstheim D. (1983), Statistical Spatial Series Modeling II: Some Further Results on Unilateral Lattice Processes. *Advances in Applied Probability*, **15**, 562-584.

Zhang N.F., Posteck M.T., Larrabee R.D., Vladar A.E., Keery W.J. and Jones S.N. (1999), Image sharpness measurement in the scanning electron microscope - Part III. *Scanning*, **21**, 246-252.